Biogeosciences Discuss., 10, 8851–8886, 2013
www.biogeosciences-discuss.net/10/8851/2013/
doi:10.5194/bgd-10-8851-2013

Biogeosciences Discussions
Open Access

Differential response of planktonic primary, bacterial, and dimethylsulfide production rates to vertically-moving and static incubations in upper mixed-layer summer sea waters

M. Galí[1], R. Simó[1], G. L. Pérez[2], C. Ruiz-González[1,*], H. Sarmento[1,], S.-J. Royer[1], A. Fuentes-Lema[3], and J. M. Gasol[1]**

[1]Institut de Ciències del Mar (CSIC), Passeig Marítim de la Barceloneta, 37–49, 08003 Barcelona, Catalonia, Spain
[2]Laboratorio de Ecología y Fotobiología Acuática (IIB-INTECH), Chascomús, Argentina
[3]Departamento de Ecoloxía e Bioloxía Animal, Facultade de Ciencias do Mar, Vigo (Pontevedra), Spain
[*]now at: Département des Sciences Biologiques, Université du Québec à Montréal, Québec, Canada
[**]now at: Federal University of Rio Grande do Norte, Department of Oceanography and Limnology, "PPg Ecologia", Natal-RN, Brazil

Received: 6 May 2013 – Accepted: 11 May 2013 – Published: 29 May 2013

Correspondence to: M. Galí (marti.gali.tapias@gmail.com)

Published by Copernicus Publications on behalf of the European Geosciences Union.

Abstract

Microbial plankton experience fluctuations in total solar irradiance and in its spectral composition as they are vertically moved by turbulence in the oceanic upper mixed layer (UML). The fact that the light exposure is not static but dynamic may have important consequences for biogeochemical processes and ocean-atmosphere fluxes. However, most biogeochemical processes other than primary production, like bacterial production or dimethylsulfide (DMS) production, are seldom measured in sunlight and even less often in dynamic light fields. We conducted four experiments in oligotrophic summer stratified Mediterranean waters, where a sample from the UML was incubated in ultraviolet (UV)-transparent bottles at three fixed depths within the UML and on a vertically-moving basket across the same depth range. We assessed the response of the phyto- and bacterioplankton community with physiological indicators based on flow cytometry singe-cell measurements, Fast Repetition Rate fluorometry (FRRf), phytoplankton pigment concentrations and particulate light absorption. Dynamic light exposure caused a disruption of the photoinhibition and photoacclimation processes associated to ultraviolet radiation (UVR), which slightly alleviated bacterial photoinhibition but did not favor primary production. Gross DMS production (GP_{DMS}) decreased sharply with depth in parallel to shortwave UVR, and displayed a dose-dependent response that mixing did not significantly disrupt. To our knowledge, we provide the first measurements of GP_{DMS} under in situ UV-inclusive optical conditions.

1 Introduction

The characteristic response times of microbial plankton match the natural variability of light exposure, which changes at different temporal scales with solar elevation, the passage of clouds, vertical mixing and even wave focusing (Gallegos and Platt, 1985). In transparent oceanic waters, exposure to high irradiance (photosynthetically available radiation, PAR) is accompanied by exposure to detrimental UVR in the upper portion

BGD
10, 8851–8886, 2013

of the water column (Vincent and Neale, 2000). Short-term irradiance fluctuations elicit fast and reversible responses (Roy, 2000), whereas continued exposure to high PAR and UVR may elicit photoacclimation (MacIntyre et al., 2002) or permanent physiological changes, i.e., irreversible damage (Buma et al., 2001).

Vertical mixing can have either a positive, neutral or negative effect on water column-integrated processes depending on the interplay between mixing rates, damage and repair kinetics, and underwater attenuation of PAR and UVR (Neale et al., 2003). In the absence of repair mechanisms, damage will be proportional to cumulative exposure (i.e., it will be dose-dependent). If moderate repair exists, mixing will allow the cells to recover in the UVR shaded portion of the UML (Fig. 1a), so that damage will no longer be dose-dependent, and a steady state will be achieved provided that the cells spend sufficient time under constant exposure conditions. In the idealized situation where damage is completely counteracted by repair in a timescale much shorter than the mixing time, or in the absence of repair, vertical mixing will have neutral effects. These responses can change with exposure time.

The effects of dynamic light exposure have concerned the aquatic photosynthesis research community for almost 40 yr (see Gallegos and Platt, 1985 and references therein), and apparently contradictory findings have often been reached using either experimental or modeling approaches (Ross et al., 2011a,b). It appears that the ability to take advantage of dynamic light exposure may depend on the taxonomic composition and size structure of the phytoplankton community, their light history, and their nutritional status (Barbieri et al., 2002; Brunet and Lavaud, 2010; Helbling and Villafañe, 2013). Knowledge on the photoresponse of (bacterial) heterotrophic activity is much more limited, but a number of studies suggest that significant PAR-driven stimulation frequently occurs (Moran et al., 2001; Church et al., 2004), as does inhibition due to UVR (Aas et al., 1996; Kaiser and Herndl, 1997). There is mounting evidence that UVR-resistance and photostimulation responses vary among bacterial phylogenetic groups (Agogué et al., 2005; Alonso-Sáez et al., 2006; Ruiz-González et al., 2012), which might be related to the occurrence of photoheterotrophic metabolisms

BGD
10, 8851–8886, 2013

in the ocean (Kolber et al., 2000; Béjà et al., 2000; Kirchman and Hanson, 2012) or to their interaction with other light-driven processes (see references in Ruiz-González et al., 2013).

Besides carbon and nutrient cycling, solar radiation modulates the biogeochemical cycles of other elements. It has recently been shown that sunlight stimulates GP_{DMS} (Galí et al., 2011) in an irradiance- and spectrum-dependent manner (Galí et al., 2013). The volatile DMS is produced mainly by the enzymatic cleavage of the phytoplankton osmolyte dimethylsulfoniopropionate (DMSP) as a result of microbial food web interactions (Simó, 2004). Marine DMS emission represents the main natural source of sulfur to the atmosphere (Lana et al., 2011) and has potential climate implications (Charlson et al., 1987) which depend on its response to solar radiation (Vallina and Simó, 2007). However, the climatic effects of DMS emission remain controversial (Quinn and Bates, 2011).

We designed an experiment where a single surface seawater sample was incubated in UVR-transparent bottles at three fixed optical depths, approximately corresponding to the water sub-surface, the optical middle, and the bottom of the UML. An additional set of bottles was regularly moved up and down across the same depth range and radiation gradient (Fig. 1; Table 1). Rather than simulating actual turbulent mixing experimentally (which is extremely difficult), vertical motion was applied as a perturbation of the photoinhibiton and photoacclimation processes occurring in upper mixing waters, with fixed-depth incubations being the static end of such perturbation. The experimental design was aimed at answering two questions: (1) photobiological: should the mixing bottles display the same response that the ones incubated at the middle optical depth considering that both treatments received a similar cumulative dose? If the response was the same this would imply that the measured processes were dose-dependent. (2) Biogeochemical and methodological: In UVR-transparent and shallow mixing layers, are the rates obtained from vertical integration of static bottle incubations equivalent to those obtained in vertically-moving bottles?

BGD
10, 8851–8886, 2013

2 Methods

2.1 Experimental setting and irradiance calculations

Surface (0.2 to 3 m deep) seawater samples were taken pre-dawn in 20–30 L polycarbonate carboys (dimmed with a black plastic bag). In the coastal experiments (C1 and C2) the samples were taken from a boat at the Blanes Bay Microbial Observatory coastal site (BBMO; 0.5 miles offshore over a water column depth of 20 m), brought to the lab, and incubated at the pier of the Barcelona Olympic Harbor during 4 h centered on the solar noon. The oceanic experiments (O1 and O2) were done in the open Mediterranean during a Lagrangian cruise over a water column depth of ca. 2000 m (R/V García del Cid). In these experiments the samples were incubated in situ, beginning 4 h before solar noon and ending 2 h after solar noon (with an intermediate sample taken after the first 2 h). In C1 and C2 mixing was applied by moving the bottle basket (Fig. 1a) manually every 15 min, completing a mixing cycle every 60 min. In the ship-based experiments the mixing bottles were continuously moved using the winch of the ship at the smallest possible vertical speed (3–4 cm s^{-1}), completing a cycle in 10–18 min. Since the waters were less transparent in the harbor than at the BBMO, in C1 and C2 the bottles were incubated at shallower depths to approximate the equivalent in situ optical depths (Table 1). Mixing layer depths (MLD) were estimated from CTD temperature profiles, and defined by a $> 0.1\,^{\circ}$C deviation with respect to 1 m depth. The buoyancy or Brunt–Väisälä frequency was calculated in 1 m bins (Fig. 2), and used as an additional criterion to distinguish the weakly-stratified UML from the more stratified waters below.

The irradiance just below the water surface (sub-surface irradiance) during the incubations was recorded with a PUV-2500 (Biospherical) multichannel filter radiometer, which was also used to measure underwater irradiance profiles in C1 and C2. In O1 and O2, the vertical profiles were measured with a PRR-800 (Biospherical). Diffuse attenuation coefficients of downward irradiance (K_d) were calculated as the linear regression between ln-transformed spectral irradiance and depth (z) in the optically homogeneous

BGD
10, 8851–8886, 2013

surface layer where the incubations were done. The time-series of sub-surface irradiance were converted to the irradiance seen by each water sample by applying the attenuation due to seawater ($e^{-K_d \cdot z}$) and the attenuation due to the incubation bottles. We used polytetrafluoroethylene (Teflon, Nalgene) bottles, which according to our measurements transmit 65 %, 77 % and 100 % of spectral irradiance in the UVB, UVA and PAR bands, respectively (Galí et al., 2013). The bottles were placed in a metallic basket which caused a minimal alteration of the tridimensional light field. For the mixing bottles, the calculation was made using a time-varying depth that corresponded to the vertical displacement of the basket. In each incubation, the mean UVB (300–320 nm) and UVA (320–400 nm) irradiance was calculated by integrating over the spectrum the mean spectral irradiance in the 6 bands measured by the PUV-2500 (centered at 305, 313, 320, 340, 380 and 395 nm) as described by Galí et al. (2013). PAR was measured in a single integrated band (400–700 nm) so that no spectral integration was required. The irradiance dose was calculated by multiplying the mean irradiance by the total incubation time.

2.2 Process measurements and analysis techniques

Primary production was measured as the ^{14}C incorporated into particles in duplicate 40 mL Teflon bottles inoculated with $NaH^{14}CO_3$ (Morán et al., 1999) and incubated in situ (including dark controls). Bacterial heterotrophic production rates were measured as ^{3}H-leucine incorporation rates (LIR; Kirchman et al., 1985; Smith and Azam, 1992) in the initial samples and on sub-samples taken from the larger (2.3 L) Teflon incubation bottles after in situ light exposure. Triplicate sub-samples plus one killed control from each Teflon bottle were further incubated for 2 h in the dark at in situ temperature in 1.5 mL eppendorf vials. In O1 and O2, incubation-averaged leucine incorporation rates (LIR) were calculated as the time-weighted average of intermediate (2 h) and final time (6 h) time incubations. In C1 and C2 leucine incorporation was also measured during "in situ" sunlit incubations in 40 mL Teflon bottles to which ^{3}H-leucine had been added.

BGD
10, 8851–8886, 2013

Samples for pigment analysis were obtained by filtering 1–2 L seawater onto GF/F filters at the beginning and the end of the incubations (O1 and O2 only). Following filtration, the filters were immediately stored in liquid nitrogen. Pigments were extracted and analysed by HPLC following Zapata et al. (2000) on a SpectraSYSTEM (Thermo) using a Waters Symmetry C8 column (150 × 4.6 mm, 3.5 µ particle size, 10 nm pore size). Calibration was made using commercial external pigment standards (DHI, Denmark), and the pigments were identified according to their elution time.

The absorption spectra of total particulate matter a_p were determined by the quantitative filter technique, using the simple transmittance method in a Lambda 800 (Perkin–Elmer) spectrophotometer. Water samples (2 L) were filtered on-board using 25 mm diameter GF/F filters. Immediately after filtration absorbance scans were measured from 350 to 750 nm at 1 nm intervals. The quantitative filter technique was applied according to NASA's optics protocols for absorption coefficient measurements (Mitchell et al., 2000). In order to minimize light scattering, the wet filters were placed as close to the spectrophotometer detector as possible and measured against a blank clean filter wetted with filtered (0.2 µm) seawater. Absorption coefficients were estimated according to the relationship $a_p(\lambda) = \frac{2.303\, A_{filter}(\lambda)\, s}{V_{filt}\, \beta(\lambda)}$ where A_{filter} is the measured absorbance, s is the clearance area of the filter, V_{filt} is the volume of filtered water, and $\beta(\lambda)$ is the amplification factor vector (Mitchell and Kiefer, 1984).

The maximum quantum yield of photosystem II photochemistry (F_v/F_m), an indicator of phytoplankton photosynthetic performance and photoinhibtion, was measured by Fast Repetition Rate fluorometry (FastTracka I, Chelsea), as detailed by Galí et al. (2013).

A FACSCalibur (Becton & Dickinson) flow cytometer equipped with a 15 mW Argon-ion laser (488 nm emission) was used to enumerate picophyto- and bacterioplankton populations and to measure their performance at the single-cell level. The cell-specific fluorescence of each different picophytoplankton population (normalized to their side scatter – SSC –, a proxy for cell size) was measured following Marie and Partensky (2006). At least 30 000 events were acquired for each sub-sample. Fluorescent

BGD
10, 8851–8886, 2013

beads (1 µm, Fluoresbrite carboxylate microspheres, Polysciences Inc., Warrington, PA) were added at a known density as internal standards. Two subpopulations of heterotrophic bacterioplankton were distinguished based on the Nucleic-Acid-Double-Staining (NADS) viability protocol: intact-membrane (or "live") bacteria and membrane-compromised (or "dead") bacteria (Grégori et al., 2001), which uses a combination of the cell-permanent nucleic acid strain SybrGreen I (Molecular Probes, Eugene, OR) and the cell-impermeant propidium iodine (PI, Sigma Chemical Co.) fluorescent probe. We used a 1 : 10 SG1 and 10 µg mL^{-1} PI concentrations that were added to live samples less than 2 h after sampling. After simultaneous addition of each stain, the samples were incubated for 20 min in the dark at room temperature and then analyzed.

DMS and DMSP were measured by purge and trap gas chromatography (Shimadzu GC14A) coupled to flame photometric detection. Net biological DMS production ($NP_{bio,DMS}$) was obtained by incubating whole water samples in 2.3 L Teflon bottles and correcting afterward for photochemical DMS loss, as described by Galí et al. (2013). Gross DMS production was measured in the same way in additional bottles amended with 200 nmol L^{-1} dimethyldisulfide (Galí et al., 2011), an effective inhibitor of bacterial DMS consumption (Wolfe and Kiene, 1993; Simó et al., 2000).

DMS photolysis was measured in 0.2 µm filtered-water incubations in 40 mL Teflon bottles or 50 mL quartz flasks. As expected, DMS photolysis was linearly related to the photochemically-weighted irradiance dose (Fig. 3). Since we observed distinct DMS photolysis yields in coastal (C1–C2) versus oceanic (O1–O2) experiments, a photolysis rate constant (k^*_{photo}) was used at each experimental location to correct the biological rates for photochemical DMS loss.

All the variables were measured in duplicate incubation bottles except DMS production rates, which require large incubation volumes to properly account for food-web processes like microzooplankton grazing (Saló et al., 2010).

BGD
10, 8851–8886, 2013

2.3 Statistical analyses

Each variable was normalized within each experiment to the vertical integral of the fixed incubations. After pooling the four experiments together we checked for significant differences among treatments. If the Bartlett's equal variance test was successfully passed ($p > 0.05$) a parametric one-way ANOVA was used. Otherwise, a non-parametric Kruskal–Wallis ANOVA was performed. After a significant ANOVA ($p < 0.05$) multiple comparisons were done with the Tukey–Kramer test.

3 Results and discussion

3.1 Oceanographic settings

The sampled upper mixed layer was in all cases exposed to high proportions of UVR, i.e. > 10 % of the sub-surface UVA and UVB levels. Only in C2 the deeper portion of the UML was exposed to < 10 % of sub-surface UVB (Fig. 2; Table 1). The phytoplankton community was typical of oligotrophic conditions, with low biomass and large contributions of the pico-sized fraction (*Prochlorococcus, Synechococcus* and picoeukaryotes) though in different proportions (Table 1). The picoeukaryote fraction was likely dominated by haptophytes (prymnesiophytes) and pelagophytes in O1 and O2 according to HPLC pigment data (Pérez et al., 2013). Diatoms in C1 and C2 and small dinoflagellates (< 10 µm) in O1 and O2 also made significant contributions to total phytoplankton biomass. The presence of strong DMSP producers, such as dinoflagellates and haptophytes, may explain the elevated DMSPt : Chl *a* ratios of 196–315 µmol g^{-1} found in the initial O1–O2 samples, compared to the 77–92 (already elevated) found in C1–C2.

The mixing layer was very shallow at the coastal site (MLD of 3–4 m). In the oceanic setting, the UML deepened from 7 m (O1) to 16 m (O2) due to the passage of a storm (Fig. 2). The fact that all experiments took place in soft wind conditions, and the relatively high values of the buoyancy (Brunt–Väisälä) frequency within the UML suggest

BGD
10, 8851–8886, 2013

that it was not mixing actively at the time of the CTD casts (Table 1). If we assume that vertical diffusivity (K_z) in the UML interior was in the range 10^{-2}–10^{-4} $m^2 s^{-1}$ (Denman and Gargett, 1983; Ross et al., 2011b), it would take between ca. 0.25 to 100 h for a population of particles released at a single depth to diffuse across one optical depth in the UML depending on the wavelengths and MLD considered (Gallegos and Platt, 1985). A similar range is obtained by calculating the mixing timescale as MLD^2/K_z as suggested by Ross et al. (2011a,b). The highest K_z might be representative of nighttime convective overturning, while the lowest K_z might be more representative of the daytime, when mixing was likely inhibited by solar heating (Brainerd and Gregg, 1995). From these calculations we conclude that the simulated mixing times were considerably faster than the actual mixing times. Although we tried to simulate the optical gradient experienced by the organisms and solutes within the UML, in practice the incubations spanned a larger optical gradient once the attenuation due to seawater and the incubation bottles was taken into account (Table 1).

Indeed, some of the differences between experiments and particularly between O1 and O2 may arise from slight differences in experimental exposure and prior light history of the plankton. Yet, our discussion will focus on the general trends rather than the differences among individual experiments.

3.2 Phytoplankton photosynthetic performance and photoacclimation

Particulate primary production (PPp) was moderately inhibited at the surface, optimal at the middle depth, and slightly lower at the bottom, with the exception of C1 (Fig. 4a). PPp in mixing bottles resembled that in surface bottles and was 18 % lower than in middle bottles except in C1 ($p < 0.01$). As a result, vertically integrated PPp from fixed bottles generally exceeded that in mixing bottles by 10–17 % (C1 excluded). This result contrasts with that obtained by Bertoni et al. (2011), who observed a neutral to positive effect of dynamic light exposure in coastal Mediterranean waters in late spring. The response of primary production may be explained by different photoacclimation,

BGD
10, 8851–8886, 2013

photoprotection and damage and repair processes that will be explored in the paragraphs below.

At the end of the incubations, the average fluorescence of *Synechococcus* and picoeukaryote cell populations was generally lowest at the surface and increased with depth (Fig. 4b, c). Fluorescence was generally lower than average in mixing bottles (although different patterns were observed for picoeukaryotes in O2). Similar responses were observed for nanoeukaryotes in C2 and for *Prochlorococcus* in O1 (data not shown), accompanied by marked decreases in *Prochlorococcus* cell counts, as previously shown by Sommaruga et al. (2005). In concordance with the response of populations analysed with single-cell techniques, bulk phytoplankton F_v/F_m tended to increase with incubation depth (Fig. 4d). F_v/F_m in mixing bottles was (again) lower than the vertical integral of fixed bottles in C1 and O1, but not in O2, potentially due to the high fluorescence yields of the picoeukaryote population (Fig. 4c). The decrease in fluorescence yields may simultaneously result from a decrease in chlorophyll *a* (Chl *a*) content per cell (MacIntyre et al., 2002), an increase in excess energy dissipation as heat by photoprotective carotenoids (non-photochemical quenching), photodamage of photosystem II, and pigment bleaching (Vincent and Neale, 2000).

Chl *a* concentrations generally increased (by 10–30 %) during the experiments except in O1, where a ca. 20 % decrease was found. In O1 and O2, the ratio of photosynthetic carotenoids to Chl *a* (PC/Chl *a*) increased with depth, from ca. 0.48 at the surface to ca. 0.56 in bottom bottles. PC/Chl *a* in mixing bottles was close to the vertical integral of fixed bottles (Fig. 4e). This suggests that phytoplankton photoacclimated during the time frame of the experiment (6 h) by adjusting PC/Chl *a* to the average spectral irradiance they were exposed to, likely seeking to optimize photosynthesis. Another physiological indicator that is worth analyzing is the ratio of photosynthetic carotenoids to non-photosynthetic carotenoids (PC/NPC; Fig. 4f), as defined by Bricaud et al. (1995). In the fixed bottles, this ratio increased from about 0.66 to 0.90 from surface to bottom. At the surface, the low PC/NPC values were due to the net synthesis of NPC (with a 20–40 % increase during the incubation). These results indicate an increasing

BGD
10, 8851–8886, 2013

investment in photoprotection through non-photochemical quenching at higher spectral irradiance. This is consistent with the decrease in photosystem II fluorescence yields (Fig. 4d), since NPC compete for excitation energy with the other energy dissipation pathways: photochemistry and fluorescence emission. Surprisingly, mixing bottles displayed the highest values of PC/NPC due to higher-than-average PC concentrations, a response that remains difficult to interpret.

The xanthophyll cycle pigments diadinoxanthin (Dd) and diatoxanthin (Dt) were up-regulated by about 35 % (up to 75 %) during the exposure relative to their initial concentration. Likewise, (Dd + Dt) concentrations relative to Chl *a* increased by 50 % in the ensemble of all treatments in O1 and O2. (Dd + Dt)/Chl *a* generally increased towards the surface, and showed intermediate values in mixing bottles (Fig. 4g). These xanthophylls constitute a photoprotective mechanism in haptophytes, dinoflagellates and diatoms (van de Poll and Buma, 2009) by which the epoxidated form (Dd) is enzymatically de-epoxidated to Dt, and vice-versa, depending on the cells' need for photoprotection. Dd assists in light harvesting and Dt is thought to thermally dissipate excess energy, so that a high value of the de-epoxidation state index Dt/(Dd + Dt) indicates a stronger need for photoprotection. The highest Dt/(Dd + Dt) were observed in surface bottles (and in the mixing bottle only in O1), with values between 0.50–0.70. However, this index must be viewed with caution because Dd to Dt interconversion can respond in a matter of minutes (i.e., faster than the filtration time after the experiment), and because UV-driven de novo Dd synthesis may also lower the Dt/(Dd + Dt) index (van de Poll and Buma, 2009). We also tried to calculate the de-epoxidation state of the violaxanthin-antheroxanthin-zeaxanthin (VAZ) cycle (a photoprotection system that operates in chlorophytes and prasinophytes) as (V+0.5A)/(V+A+Z) following Sobrino et al. (2005). However, we did not find meaningful trends in this index, perhaps because an active xanthophyll cycle is not found in cyanobacteria (*Synechococcus*) and prochlorophytes although they contain de-epoxidated xanthophylls (van de Poll and Buma, 2009).

BGD
10, 8851–8886, 2013

UV-absorbing (sunscreen) compounds, possibly mycosporine-like aminoacids (Shick and Dunlap, 2002), were observed in particulate absorption spectra in O1 and O2 (Fig. 4i). The ratio of particulate light absorption at 340 nm relative to that at the blue peak of Chl *a* at 440 nm, $a_{p,340}/a_{p,440}$ was highest (1–1.5) in surface bottles and lower (0.7–0.8) in middle and bottom bottles. Mixing bottles showed an ambiguous response, with low $a_{p,340}/a_{p,440}$ in O1 and slightly higher $a_{p,340}/a_{p,440}$ in O2.

The several photoresponse indicators we have explored indicate that, although phytoplankton deployed different photoprotection mechanisms, these were not enough to counteract high PAR and UV-driven photoinhibition in surface bottles. Seen another way, the investment in photoprotection might have decreased the allocation of resources to carbon fixation. In middle bottles, conversely, the combination of high PAR and longwave UVA (which can also be used for photosynthesis, Helbling et al., 2003) and a lower investment in photoprotection due to lower proportions of UVR resulted in optimal PPp. It is also important to bear in mind that different phytoplankton groups likely preferred different photoprotection mechanisms within those cited.

The response of mixing bottles is more difficult to interpret. The reduced photosynthetic performance in C2, O1 and O2 might indicate that the short surface exposure received by mixing bottles was enough to cause some irreversible inhibition, and that phytoplankton repair capacity was limited. However, this is not clearly supported by radiative stress indicators. In addition, repair is thought to be more efficient at elevated temperatures like those encountered in our study (Campbell et al., 1998; van de Poll and Buma, 2009). The fact that surface inhibition was only moderate and that highest PPp occurred in the middle bottle suggests that the photosynthetic machinery of phytoplankton was well adapted to a stratified system and thus not geared to take advantage of fast changes in spectral irradiance. This contrasts with what has been found for coastal tropical phytoplankton thriving in turbid waters (Helbling et al., 2003) or even for coastal Mediterranean assemblages in late spring (Bertoni et al., 2011).

BGD
10, 8851–8886, 2013

3.3 Response of bacterial heterotrophic production

In fixed bottle incubations, LIR were significantly inhibited at the surface by 14–28 % with respect to the vertical integral (except in C1), and increased with depth to find their optimum at the bottom of the mixed layer (Fig. 5a). LIR in mixing bottles resembled those of bottom bottles in 3 out of 4 experiments, and were higher (though not significantly) than those in middle bottles and the vertical integral. This suggests that fast mixing favored recovery and photorepair over photodamage. It is well known that photolyase enzymes use UVA and blue light to repair damaged DNA. According to Kaiser and Herndl (1997), optimal photoreactivation occurs in a certain window of UVA/UVB that, in our experiments, would roughly correspond to the bottom half of the UML (Fig. 1b). This interpretation is supported by the higher proportions of intact-membrane bacteria found in mixing bottles at the end of the incubations with respect to the surface bottles (O1 and O2 only; Fig. 5c). Yet, the vertical trend shown by this cytometric indicator in fixed bottles contradicts this view, especially in O2, where the proportion of intact-membrane bacteria decreased with depth.

In addition to the post-exposure dark incubations, in C1 and C2 we measured LIR during the sunlit incubations, i.e., with the ^{3}H-leucine added into exposed bottles (Fig. 5b). In these in situ incubations, surface and mixing bottles displayed more similar degrees of inhibition, and the trends of bacterial production with depth did not match those found in post-exposure dark incubations. We also measured LIR in aluminum foil-darkened bottles placed in the in situ incubation basket. Dark LIR was 22 % higher than the vertical integral of sunlit bottles in C1, but no differences were observed in C2 (Fig. 5b). The discrepancies between in situ and post-exposure leucine incorporation may be due to distinct photoinhibition and photorepair dynamics during sunlit and dark incubations, i.e., we do not know how much of the substrate was taken up before the onset of photoinhibition during in situ exposure, or how long the photoinhibition lasted during post-exposure dark incubations. These methodological issues might be overcome with the development of sensitive methods that allowed a faster determination

BGD
10, 8851–8886, 2013

of bacterial heterotrophic production, which is particularly challenging in oligotrophic waters with low activity.

Different explanations have been invoked to explain the changes in bacterial activity under sunlight. For instance, the occurrence of photoheterotrophic metabolisms in some bacterial groups, or the exudation of labile organic matter by phytoplankton at high irradiance (see review by Ruiz-González et al., 2013). Unfortunately, we did not investigate the phylogenetic composition of the bacterial communities in our experiments. No obvious patterns linking the response of LIR and PPp were found, perhaps because phytoplankton-bacteria interactions through the dissolved carbon pool are complex and group-specific (Sarmento and Gasol, 2012). Despite the numerous uncertainties, our study adds valuable information to the only previous study of bacterial production under dynamic light exposure (Bertoni et al., 2011), and agrees with that work in that the effect of mixing was neutral to positive compared to fixed incubations.

3.4 Response of gross DMS production

Gross DMS production showed the strongest vertical gradient among the three processes, and increased significantly by about three-fold between the bottom and the surface of the UML in fixed incubations (Fig. 6a). Gross and DMS production in mixing bottles was not significantly different from that in middle bottles, and not either from the vertical integral, although a slight trend towards lower GP in mixing bottles occurred in C1 and C2.

Gross DMS production results from the addition and interaction of several processes, namely: exudation of DMS by phytoplankton, bacterial degradation of DMSP released by phytoplankton as a result of grazing, viral infection, or cell death, and even the reduction of dimethylsulfoxide (Spiese et al., 2009; Asher et al., 2011). Galí et al. (2013) showed that UVR stimulates GP_{DMS} in a spectral irradiance-dependent manner, a result that is confirmed by our present study. They also demonstrated that the stimulation is more effective at shorter and more energetic UVR wavelengths, with a spectral peak around 330 nm, and attributed the stimulation effect to phytoplankton DMS release

BGD
10, 8851–8886, 2013

caused by the additive effects of excess PAR (Stefels, 2000) and UVR stress (Sunda et al., 2002). Furthermore, it was suggested that lethal UVR exposure could promote DMS production as a result of phytoplankton cell lysis and subsequent DMSP release. This mechanism would make more DMSP available to bacteria and to algal DMSP cleavage enzymes ("lyases") released along with algal DMSP.

In the ensemble of all the experiments, experiment-normalized PPp and GP_{DMS} were weakly but significantly correlated (Pearson's $r = -0.58$; $p = 0.018$; Spearman's $\rho = -0.51$; $p = 0.044$). Moreover, the response of GP_{DMS} to radiative stress was generally consistent with the patterns of photoinhibition and photoprotection. Whether or not this response was the result of active physiological regulation of phytoplankton cells remains to be elucidated. Clearly, better methods are needed to study the relative weight of different DMS production processes and their modulation by spectral irradiance (Galí et al., 2013). Sunda et al. (2002) suggested that intracellular DMSP cleavage to DMS and further oxidation products might help phytoplankton cells coping with oxidative stress. Our data suggest that, even if GP_{DMS} arose completely from intracellular DMSP cleavage (which is very unlikely), this potential antioxidant mechanism would not be enough to counteract photoinhibition and ameliorate photosynthetic performance, even if working in tandem with other photoprotection mechanisms.

DMSP concentrations displayed only moderate changes (< 5 % variation in 13 out of 16 incubations) and no clear trends were found across treatments (data not shown). A strong DMSP depletion in surface bottles was only found in O2 (21 %). The stability of the DMSP concentration across spectral irradiance treatments is notable, given that (1) a lower amount of fixed carbon was available for DMSP synthesis in surface and mixing samples, and (2) higher amounts of DMSP were lost as DMS (and perhaps as DMSP) at higher irradiance. The quotient of GP_{DMS} to DMSPt was $0.42\,d^{-1}$, $0.29\,d^{-1}$, $0.18\,d^{-1}$, and $0.21\,d^{-1}$ on average in surface, middle, bottom and mixing bottles, respectively. These data suggest that DMSP turnover was more active at high irradiance, and therefore faster DMSP synthesis was required to sustain DMSP concentrations. Gross DMSP synthesis rates were not measured in our experiments, but, interestingly,

BGD
10, 8851–8886, 2013

experiment-normalized net DMSP synthesis rates and PPp were correlated (Pearson's $r = 0.50$; $p = 0.048$; Spearman's $\rho = 0.65$; $p = 0.006$). Recent results suggest that DMS can be produced intracellularly in phytoplankton through DMSP cleavage by OH radicals, without the need of DMSP cleavage enzymes (D. J. Kieber, personal communication, 2012). In this case, intracellular DMSP would be a more effective radical scavenger than previously thought (Sunda et al., 2002), and this could explain why such an important proportion of the intracellular DMSP pool escapes as DMS without reacting with intracellular oxidants.

Net biological DMS production ($NP_{bio,DMS}$) showed a pattern similar to that of GP_{DMS} (Fig. 6b). This variable is interesting in that it tells the net effect of sunlight on biological DMS cycling, that is, on the difference between GP_{DMS} and bacterial DMS consumption. Bacterial DMS consumption rates, calculated by subtracting $NP_{bio,DMS}$ from GP_{DMS}, consumed on average 11 %, 31 %, 43 % and 14 % of GP_{DMS} in surface, middle, bottom and mixing bottles, respectively. Thus, the imbalance between GP_{DMS} and bacterial DMS consumption increased with spectral irradiance due to UV and/or PAR inhibition of bacterial DMS consumption and stimulation of GP_{DMS}, making the vertical gradient of $NP_{bio,DMS}$ even larger than that of GP_{DMS} (Fig. 6b). The net stimulating effect of sunlight on biological DMS production was largely compensated by DMS photolysis, so that net overall DMS concentration changes were close to zero in all treatments, as already observed by Galí et al. (2013) with other experimental settings.

Bacterial DMS consumption, expressed as the % of vertically-integrated rates, was 49, 79, 125 and 78 in surface, middle, bottom and mixing bottles, respectively. Although these results suffer from a large uncertainty due to error propagation, they suggest that bacterial DMS consumption was more strongly inhibited than bulk LIR, and that it was photoinhibited in a dose-dependent manner. Severe photoinhibition was already observed by Toole et al. (2006), who observed a similar response of bacterial DMS consumption and LIR. Since only a portion of the bacterial community is able to consume DMS through oxidation, it is likely that the photoresponse of bacterial DMS consumers and that of bulk heterotrophic bacteria differ (as suggested by Galí and Simó, 2010)

BGD
10, 8851–8886, 2013

or even that the photoresponse of different metabolic activities differs in a given cell or strain. Clearly, these issues deserve further investigation.

3.5 Differential irradiance- and dose-response among biogeochemical processes

The experiment-normalized PPp, LIR and community DMS production rates were plotted against the mean (UVB, UVA, PAR) incubation irradiance in the ensemble of all the experiments, and the points corresponding to fixed bottles were fitted with a linear regression (Fig. 7). We also calculated the Pearson correlation coefficient between the experiment-normalized process rates and (1) mean irradiance and (2) total irradiance dose for each radiation band (Fig. 8). The aim of this exercise was to identify whether a process was more dose-dependent or irradiance ("dosage-rate")-dependent, following the rationale exposed in the Introduction. Note that in our experimental setting it is hard to discriminate between the effects of each band of the spectrum, since the proportion of shortwave UV decreases along with total (or PAR) irradiance as we move deeper in the water column.

PPp showed a slight negative trend with respect to irradiance in fixed bottles in the three radiation bands, which was mainly driven by photoinhibition in surface bottles. In fact, the response was rather flat below an irradiance threshold of ca. 0.4 $W m^{-2}$ UVB, 16 W^{-2} UVA and 1000 µmol photons $m^{-2} s^{-1}$. The correlation with irradiance was higher than that with dose (Fig. 8a), suggesting that some balance between inhibition and protection/repair could be attained in the different exposure regimes. The highest linear correlation was found with UVA irradiance, perhaps indicating that this band drives photoinhibition in UV-transparent waters. In concordance with this suggestion, some studies have shown that the spectral peak of UV photoinhibition occurs in the UVA, due to the combination of increasing irradiance and decreasing UV efectiveness as we move towards longer wavelengths (Neale and Kieber, 2000).

LIR decreased with increasing UVB, UVA and PAR with a slope very similar to that of PPp. Contrary to the other processes examined, the photoinhibition of LIR was more

BGD
10, 8851–8886, 2013

strongly correlated to the dose than to irradiance (Fig. 8b), particularly in the UVB band, suggesting that cumulative UVB-induced DNA damage occurred in bacterial cells in fixed incubations (Buma et al., 2001). This fits with the general idea that the radiation bands causing damage (UVB) elicit more dose-dependent responses than the radiation bands that are used by the cells to conduct physiological processes (PAR and longwave UVA).

Community DMS production rates showed a strong response to variations in spectral irradiance, with a steeper slope observed for $NP_{bio,DMS}$ than for GP_{DMS} (Fig. 7c, d). The strongest correlations were found between GP_{DMS} and irradiance in the three bands, particularly in the UVA. This agrees with previous studies that suggested, using distinct approaches, that the spectral peak of sunlight-induced DMS production occurs in the 330–340 nm region in surface UV-transparent waters (Toole et al., 2008; Levine et al., 2012; Galí et al., 2013).

Finally, note that among all process and radiation combinations the correlation was stronger when mixing bottles were excluded. This illustrates in a loose way that mixing disrupted the photoacclimation and photodamage processes, as thoroughly discussed in Sects. 3.2–3.4.

4 Conclusions

The photoresponse of phytoplankton, bacterioplankton, and community DMS production displayed clear trends in bottles incubated at fixed depths in the UML (Fig. 7) despite the relatively small gradient in spectral irradiance. The irradiance dose-response in mixing bottles was distinct (though subtle) in each of the processes measured, as well as for different physiological indicators. In the oligotrophic waters investigated, dynamic light exposure *generally* caused, compared to the middle bottles receiving the same cumulative exposure (1) an adverse though non significant effect on particulate primary production, concomitant with reduced cell-specific fluorescence in most experiments and phytoplankton groups; (2) a slightly alleviating effect on bacterial production

BGD
10, 8851–8886, 2013

photoinhibition, related to an increase in the proportion of intact-membrane or "live" heterotrophic bacteria in two of the experiments; and (3) a neutral effect or slight reduction in gross DMS production. These responses translated, in some experiments, into measurable deviations with respect to the vertically-integrated rates in the water column; in others, the effects were close to neutral or too small to be reliably detected. Incubating the samples at a fixed intermediate optical depth appears as a reasonable and convenient solution for measuring GP_{DMS} and leucine incorporation, at least in UVR-transparent stratified UML waters. However, this solution might not be optimal for measuring UML-integrated primary production. Our results call for a more systematic assessment of the consequences of dynamic light exposure of microbial plankton in different oceanic regimes. This way, the photobiological processes governing, among other important processes, the ocean-atmosphere exchange of long-lived (CO_2) and short-lived (DMS) gases of climatic relevance will be better understood.

Acknowledgements. We thank the staff at Port Olímpic de Barcelona for their collaboration, and the crew and scientists aboard R/V García del Cid for their invaluable help in setting up the experiments during the SUMMER-I cruise. We also thank David J. Kieber for his insightful comments on an earlier version of the manuscript. M. G. acknowledges the receipt of a CSIC JAE scholarship. This work was supported by the (former) Spanish Ministry of Science and Innovation through the project SUMMER (CTM2008-03309/MAR). This is a contribution of the Research Groups on Marine Biogeochemistry and Global Change and on Aquatic Microbial Food Webs, supported by the Generalitat de Catalunya.

References

Aas, P., Lyons, M., Pledger, R., Mitchell, D., and Jeffrey, W.: Inhibition of bacterial activities by solar radiation in nearshore waters and the Gulf of Mexico, Aquat. Microb. Ecol., 11, 229–238, doi:10.3354/ame011229, 1996. 8854

Agogué, H., Joux, F., Obernosterer, I., and Lebaron, P.: Resistance of marine bacterioneuston to solar radiation, Appl. Environ. Microb., 71, 5282–5289, doi:10.1128/AEM.71.9.5282-5289.2005, 2005. 8854

BGD
10, 8851–8886, 2013

Alonso-Sáez, L., Gasol, J. M., Lefort, T., Hofer, J., and Sommaruga, R.: Effect of natural sunlight on bacterial activity and differential sensitivity of natural bacterioplankton groups in northwestern Mediterranean coastal waters, Appl. Environ. Microb., 72, 5806–5813, doi:10.1128/AEM.00597-06, 2006. 8854

Asher, E. C., Dacey, J. W. H., Mills, M. M., Arrigo, K. R., and Tortell, P. D.: High concentrations and turnover rates of DMS, DMSP and DMSO in Antarctic sea ice, Geophys. Res. Lett., 38, 1–5, doi:10.1029/2011GL049712, 2011. 8866

Barbieri, E. S., Villafañe, V. E., Helbling, E. W., and Nov, N.: Experimental Assessment of UV Effects on Temperate Marine Phytoplankton When Exposed to Variable Radiation Regimes Experimental assessment of UV effects on temperate marine phytoplankton when exposed to variable radiation regimes, Limnol. Oceanogr., 47, 1648–1655, 2002. 8854

Béjà, O., Aravind, L., Koonin, E. V., Suzuki, M. T., Hadd, A., Nguyen, L. P., Jovanovich, S. B., Gates, C. M., Feldman, R. A., Spudich, J. L., Spudich, E. N., and DeLong, E. F.: Bacterial Rhodopsin: evidence for a new type of phototrophy in the sea, Science, 289, 1902–1906, doi:10.1126/science.289.5486.1902, 2000. 8855

Bertoni, R., Jeffrey, W. H., Pujo-Pay, M., Oriol, L., Conan, P., and Joux, F.: Influence of water mixing on the inhibitory effect of UV radiation on primary and bacterial production in Mediterranean coastal water, Aquat. Sci., 73, 377–387, doi:10.1007/s00027-011-0185-8, 2011. 8861, 8864, 8866

Brainerd, K. and Gregg, M.: Surface mixed and mixing layer depths, Deep-Sea Res. Pt. I, 42, 1521–1543, 1995. 8861

Bricaud, A., Babin, M., Morel, A., and Claustre, H.: Variability in the chlorophyll-specific absorption coefficients of natural phytoplankton: analysis and parameterization, J. Geophys. Res.-Oceans, 100, 13321–13332, doi:10.1029/95JC00463, 1995. 8862

Brunet, C. and Lavaud, J.: Can the xanthophyll cycle help extract the essence of the microalgal functional response to a variable light environment?, J. Plankton Res., 32, 1609–1617, doi:10.1093/plankt/fbq104, 2010. 8854

Buma, A. G., Helbling, E. W., de Boer, M. K., and Villafañe, V. E.: Patterns of DNA damage and photoinhibition in temperate South-Atlantic picophytoplankton exposed to solar ultraviolet radiation, J. Photoch. Photobio. B, 62, 9–18, 2001. 8854, 8870

Campbell, D., Eriksson, M. J., Oquist, G., Gustafsson, P., and Clarke, A. K.: The cyanobacterium *Synechococcus* resists UV-B by exchanging photosystem II reaction-center D1 proteins, P. Natl. Acad. Sci. USA, 95, 364–9, 1998. 8864

BGD
10, 8851–8886, 2013

Charlson, R., Lovelock, J., Andreae, M., and Warren, S.: Oceanic phytoplankton, atmospheric sulphur, cloud albedo and climate, Cah. Rev. The., 326, 655–661, 1987. 8855

Church, M. J., Ducklow, H. W., and Karl, D. M.: Light dependence of [^{3}H]leucine incorporation in the oligotrophic North Pacific ocean, Appl. Environ. Microb., 70, 4079–4087, doi:10.1128/AEM.70.7.4079-4087.2004, 2004. 8854

Denman, K. L. and Gargett, A. E.: Time and space scales of vertical mixing in the upper ocean, Limnol. Oceanogr., 28, 801–815, 1983. 8861

Galí, M. and Simó, R.: Occurrence and cycling of dimethylated sulfur compounds in the Arctic during summer receding of the ice edge, Mar. Chem., 122, 105–117, doi:10.1016/j.marchem.2010.07.003, 2010. 8868

Galí, M., Saló, V., Almeda, R., Calbet, A., and Simó, R.: Stimulation of gross dimethylsulfide (DMS) production by solar radiation, Geophys. Res. Lett., 38, 1–5, doi:10.1029/2011GL048051, 2011. 8855, 8859

Galí, M., Ruiz-González, C., Lefort, T., Gasol, J. M., Cardelús, C., Romera-Castillo, C., and Simó, R.: Spectral dependence of sunlight effects on plankton dimethylsulfide production, Limnol. Oceanogr., 58, 489–504, 2013. 8855, 8857, 8858, 8859, 8866, 8867, 8868, 8870, 8881

Gallegos, C. L. and Platt, T.: Vertical advection of phytoplankton and productivity estimates: a dimensional analysis, Mar. Ecol.-Prog. Ser., 26, 125–134, 1985. 8853, 8854, 8861

Grégori, G., Citterio, S., Ghiani, A., Labra, M., Sgorbati, S., Brown, S., and Denis, M.: Resolution of viable and membrane-compromised bacteria in freshwater and marine waters based on analytical flow cytometry and nucleic acid double staining, Appl. Environ. Microb., 67, 4662–4670, 2001. 8859

Helbling, E. W., Gao, K., Gonçalves, R., Wu, H., and Villafañe, V. E.: Utilization of solar UV radiation by coastal phytoplankton assemblages off SE China when exposed to fast mixing, Mar. Ecol.-Prog. Ser., 259, 59–66, doi:10.3354/meps259059, 2003. 8864

Helbling, E. W., Carrillo, P., Medina-Sánchez, J. M., Durán, C., Herrera, G., Villar-Argaiz, M., and Villafañe, V. E.: Interactive effects of vertical mixing, nutrients and ultraviolet radiation: in situ photosynthetic responses of phytoplankton from high mountain lakes in Southern Europe, Biogeosciences, 10, 1037–1050, doi:10.5194/bg-10-1037-2013, 2013. 8854

Kaiser, E. and Herndl, G. J.: Rapid recovery of marine bacterioplankton activity after inhibition by UV radiation in coastal waters, Appl. Environ. Microb., 63, 4026–4031, 1997. 8854, 8865, 8879

BGD
10, 8851–8886, 2013

Kirchman, D. L. and Hanson, T. E.: Bioenergetics of photoheterotrophic bacteria in the oceans, Environ. Microbiol. Rep., 5, 188–199, doi:10.1111/j.1758-2229.2012.00367.x, 2012. 8855
Kirchman, D., K'nees, E., and Hodson, R.: Leucine incorporation and its potential as a measure of protein synthesis by bacteria in natural aquatic systems, Appl. Environ. Microb., 49, 599–607, 1985. 8857
Kolber, Z., Van Dover, C., Niederman, R., and Falkowski, P.: Bacterial photosynthesis in surface waters of the open ocean, Cah. Rev. The., 407, 177–179, 2000. 8855
Lana, A., Bell, T. G., Simó, R., Vallina, S. M., Ballabrera-Poy, J., Kettle, A. J., Dachs, J., Bopp, L., Saltzman, E. S., Stefels, J., Johnson, J. E., and Liss, P. S.: An updated climatology of surface dimethlysulfide concentrations and emission fluxes in the global ocean, Global Biogeochem. Cy., 25, 1–17, doi:10.1029/2010GB003850, 2011. 8855
Levine, N. M., Varaljay, V. A., Toole, D. A., Dacey, J. W. H., Doney, S. C., and Moran, M. A.: Environmental, biochemical and genetic drivers of DMSP degradation and DMS production in the Sargasso Sea, Environ. Microbiol., 14, 1210–1223, doi:10.1111/j.1462-2920.2012.02700.x, 2012. 8870
MacIntyre, H. L., Kana, T. M., Anning, T., and Geider, R. J.: Photoacclimation of photosynthesis irradiance response curves and photosynthetic pigmentspigments in microalgae and cyanobacteria, J. Phycol., 38, 17–38, 2002. 8854, 8862
Marie, D. and Partensky, F.: Analyse de micro-organismes marins, in: La Cytométrie en Flux, edited by: Ronot, X., Grunwald, D., Mayol, J. F., and Boutonnat, J., Lavoisier, 211–233, 2006. 8858
Mitchell, B. G. and Kiefer, D. A.: Determination of absorption and fluorescence excitation spectra for phytoplankton, in: Marine Phytoplankton and Productivity, edited by: Holm-Hansen, O., Bolis, L., and Gilles, R., Springer, 157–169, 1984. 8858
Mitchell, B. G., Bricaud, A., Carder, K., Cleveland, J., Ferrari, G., Gould, R., Kahru, M., Kishino, M., Maske, H., Moisan, T., Moore, L., Nelson, N., Phinney, D., Reynolds, R., Sosik, H., Stramski, D., Tassan, S., Trees, C., Weidemann, A., Weiland, J., and Vodacek, A.: Determination of spectral absorption coefficients of particles, dissolved material and phytoplankton for discrete water samples, in: Ocean Optics Protocols for Satellite Ocean Color Sensor Validation, Revision 2, edited by: Fargion, G., Mueller, J., and McClain, C., NASA, 125–153, 2000. 8858
Morán, X. A. G., Gasol, J. M., Arin, L., and Estrada, M.: A comparison between glass fiber and membrane filters for the estimation of phytoplankton POC and DOC production, Mar. Ecol.-Prog. Ser., 187, 31–41, 1999. 8857

BGD
10, 8851–8886, 2013

Moran, X. A. G., Massana, R., and Gasol, J. M.: Light conditions affect the measurement of oceanic bacterial production via leucine uptake, Appl. Environ. Microb., 67, 3795–3801, doi:10.1128/AEM.67.9.3795-3801.2001, 2001. 8854

Neale, P. J. and Kieber, D. J.: Assessing biological and chemical effects of UV in the marine environment: spectral weighting functions, Issues in Environmental Science and Technology, 2000. 8869

Neale, P. J., Helbling, E. W., and Zagarese, H. E.: Modulation of UVR exposure and effects by vertical mixing and advection, in: UV Effects in Aquatic Organisms and Ecosystems, chap. 4, Royal Society of Chemistry, 107–134, 2003. 8854

Quinn, P. K. and Bates, T. S.: The case against climate regulation via oceanic phytoplankton sulphur emissions, Cah. Rev. The., 480, 51–6, doi:10.1038/nature10580, 2011. 8855

Ross, O. N., Geider, R. J., Berdalet, E., Artigas, M. L., and Piera, J.: Modelling the effect of vertical mixing on bottle incubations for determining in situ phytoplankton dynamics. I. Growth rates, Mar. Ecol.-Prog. Ser., 435, 13–31, doi:10.3354/meps09193, 2011a. 8854, 8861

Ross, O. N., Geider, R. J., and Piera, J.: Modelling the effect of vertical mixing on bottle incubations for determining in situ phytoplankton dynamics. II. Primary production, Mar. Ecol.-Prog. Ser., 435, 33–45, doi:10.3354/meps09194, 2011b. 8854, 8861

Roy, S.: The strategies for minimization of UV damage, in: The Effects of UV Radiation in the Marine Environment, chap. 3, edited by: de Mora, S. J., Demers, S., and Vernet, M., Cambridge University Press, Cambridge, 177–205, 2000. 8854

Ruiz-González, C., Galí, M., Lefort, T., Cardelús, C., Simó, R., and Gasol, J. M.: Annual variability in light modulation of bacterial heterotrophic activity in surface northwestern Mediterranean waters, Limnol. Oceanogr., 57, 1376–1388, doi:10.4319/lo.2012.57.5.1376, 2012. 8854

Ruiz-González, C., Simó, R., Sommaruga, R., and Gasol, J. M.: Away from darkness: a review on the effects of solar radiation on heterotrophic bacterioplankton activity, Front. Microbiol., 4, 131, doi:10.3389/fmicb.2013.00131, 2013. 8855, 8866

Saló, V., Simó, R., and Calbet, A.: Revisiting the dilution technique to quantify the role of microzooplankton in DMS(P) cycling: laboratory and field tests, J. Plankton Res., 32, 1255–1267, doi:10.1093/plankt/fbq041, 2010. 8859

Sarmento, H. and Gasol, J. M.: Use of phytoplankton-derived dissolved organic carbon by different types of bacterioplankton, Environ. Microbiol., 14, 2348–2360, doi:10.1111/j.1462-2920.2012.02787.x, 2012. 8866

BGD
10, 8851–8886, 2013

Shick, J. M. and Dunlap, W. C.: Mycosporine-like amino acids and related Gadusols: biosynthesis, acumulation, and UV-protective functions in aquatic organisms, Annu. Rev. Physiol., 64, 223–62, doi:10.1146/annurev.physiol.64.081501.155802, 2002. 8864

Simó, R.: From cells to globe: approaching the dynamics of DMS(P) in the ocean at multiple scales, Can. J. Fish. Aquat. Sci., 61, 673–684, doi:10.1139/F04-030, 2004. 8855

Simó, R., Pedrós-Alió, C., Malin, G., and Grimalt, J. O.: Biological turnover of DMS, DMSP and DMSO in contrasting open-sea waters, Mar. Ecol.-Prog. Ser., 203, 1–11, doi:10.3354/meps203001, 2000. 8859

Smith, D. C. and Azam, F.: A simple, economical method for measuring bacterial protein synthesis rates in seawater using ^{3}H-leucine, Mar. Microb. Food Webs, 6, 107–114, 1992. 8857

Sobrino, C., Neale, P. J., Montero, O., and Lubián, L. M.: Biological weighting function for xanthophyll de-epoxidation induced by ultraviolet radiation, Physiol. Plantarum, 125, 41–51, doi:10.1111/j.1399-3054.2005.00538.x, 2005. 8863

Sommaruga, R., Hofer, J. S., Alonso-Sáez, L., and Gasol, J. M.: Differential sunlight sensitivity of picophytoplankton from surface Mediterranean coastal waters, Appl. Environ. Microb., 71, 2154–2157, doi:10.1128/AEM.71.4.2154-2157.2005, 2005. 8862

Spiese, C., Kieber, D. J., Nomura, C., and Kiene, R. P.: Reduction of dimethylsulfoxide to dimethylsulfide by marine phytoplankton, Limnol. Oceanogr., 54, 560–570, 2009. 8866

Stefels, J.: Physiological aspects of the production and conversion of DMSP in marine algae and higher plants, J. Sea Res., 43, 183–197, doi:10.1016/S1385-1101(00)00030-7, 2000. 8867

Sunda, W., Kieber, D. J., Kiene, R. P., and Huntsman, S.: An antioxidant function for DMSP and DMS in marine algae, Cah. Rev. The., 418, 317–20, doi:10.1038/nature00851, 2002. 8867, 8868

Toole, D. A., Slezak, D., Kiene, R. P., Kieber, D. J., and Siegel, D. A.: Effects of solar radiation on dimethylsulfide cycling in the western Atlantic Ocean, Deep-Sea Res. Pt. I, 53, 136–153, 2006. 8868

Toole, D. A., Siegel, D. A., and Doney, S. C.: A light-driven, one-dimensional dimethylsulfide biogeochemical cycling model for the Sargasso Sea, J. Geophys. Res., 113, 1–20, doi:10.1029/2007JG000426, 2008. 8870

Vallina, S. M. and Simó, R.: Strong relationship between DMS and the solar radiation dose over the global surface ocean, Science, 315, 506–508, doi:10.1126/science.1133680, 2007. 8855

BGD
10, 8851–8886, 2013

van de Poll, W. H. and Buma, A. G. J.: Does ultraviolet radiation affect the xanthophyll cycle in marine phytoplankton?, Photoch. Photobio. Sci., 8, 1295–1301, doi:10.1039/B904501E, 2009. 8863, 8864

Vincent, W. F. and Neale, P. J.: Mechanisms of UV damage to aquatic organisms, in: The Effects of UV Radiation in the Marine Environment, chap. 6, edited by: de Mora, S. J., Demers, S., and Vernet, M., Cambridge University Press, Cambridge, 149–176, 2000. 8854, 8862

Wolfe, G. and Kiene, R. P.: Radioisotope and chemical inhibitor measurements of dimethyl sulfide consumption rates and kinetics in estuarine waters, Mar. Ecol.-Prog. Ser., 99, 261–269, 1993. 8859

Zapata, M., Rodríguez, F., and Garrido, J. L.: Separation of chlorophylls and carotenoids from marine phytoplankton: a new HPLC method using a reversed phase C8 column and pyridine-containing mobile phases, Mar. Ecol.-Prog. Ser., 195, 29–45, doi:10.3354/meps195029, 2000. 8858

BGD
10, 8851–8886, 2013

Table 1. Summary of initial sample characteristics, ecosystem settings and experimental conditions. GP_{DMS} and $NP_{bio,DMS}$ stand for gross and net biological DMS production, respectively. Pro: *Prochlorococcus*; Syn: *Synechococcus*; PPeuk: photosynthetic picoeukaryotes; Diat: diatoms; Dino: dinoflagellates; Hapto: haptophytes. See text for other abbreviations.

Experiment code	Coastal 1 (C1)	Coastal 2(C2)	Oceanic 1 (O1)	Oceanic 2 (O2)
Date	27 Jul 2010	29 Jul 2010	16 Sep 2011	20 Sep 2011
Sampling position	41.67° N, 2.81° E		40.9° N, 2.67° E	40.9° N, 2.44° E
Physical characteristics of the upper mixed layer				
SST (°C)	23.0	22.7	25.2	23.6
MLD (m)	4	3	7	16
Z 10 % 320 nm	7	7	12	11
Z 10 % 380 nm	20	20	38	32
Buoyancy frequency (h^{-1})	6.2 ± 1.7	8.8 ± 2.7	8.1 ± 2.8	4.9 ± 0.9
Wind speed ($m\,s^{-1}$)	2.4–6.7	1.4 –7.1	0.3–4.8	1.0–9.5
UVB range ($W\,m^{-2}$)	0.4–1.4	0.4–1.1	0.3–1.1	0.04–1.1
UVA range ($W\,m^{-2}$)	22–37	21–31	19–30	9–30
PAR range ($\mu mol\,photons\,m^{-2}\,s^{-1}$)	1100–1580	1010–1330	830–1360	410–1340
Experimental conditions				
Incubation depth (m)	0.3, 1, 3	0.5, 1.5, 3.5	0.5, 3, 11	0.5, 5.5, 18
Equivalent depth UVB (m)	1.3, 4, 10	1.3, 3.5, 6	2.5, 5, 13	2.5, 7, 20
Mixing time (min)	60	60	10	18
UVB range ($W\,m^{-2}$)	0.04–0.9	0.13–0.7	0.09–0.7	0.01–0.65
UVA range ($W\,m^{-2}$)	4–28	9–24	11–23	5–22
PAR range ($\mu mol\,photons\,m^{-2}\,s^{-1}$)	460–1930	600–1210	610–1360	320–1290
Initial sample characteristics				
DMS ($nmol\,L^{-1}$)	7.5	8.5	2.1	2.1
DMSPt ($nmol\,L^{-1}$)	23.0	18.5	18.2	19.6
Chl *a* ($\mu g\,L^{-1}$)	0.24	0.25	0.08	0.08
Dominant phytoplankton (biomass)	PPeuk > Diat > Pro		Syn > Dino > PPeuk (Hapto)	
Bacteria (10^5 cells mL^{-1})	9.0	7.3	9.4	7.3
Intact-membrane bacteria (%)	54	52	56	56
Biogeochemical process rates (min–max)				
PPp ($nmol\,C\,L^{-1}\,h^{-1}$)	80–150	160–200	20–26	21–25
LIR t_0 ($pmol\,leu\,L^{-1}\,h^{-1}$)	32	21	36	18
LIR ($pmol\,leu\,L^{-1}\,h^{-1}$)	33–37	16–21	37–44	17–27
GP_{DMS} ($nmol\,DMS\,L^{-1}\,h^{-1}$)	0.05–0.40	0.24–0.49	na	0.07–0.17
$NP_{bio,DMS}$ ($nmol\,DMS\,L^{-1}\,h^{-1}$)	0.03–0.32	0.18–0.44	0.02–0.10	0.04–0.16

BGD
10, 8851–8886, 2013

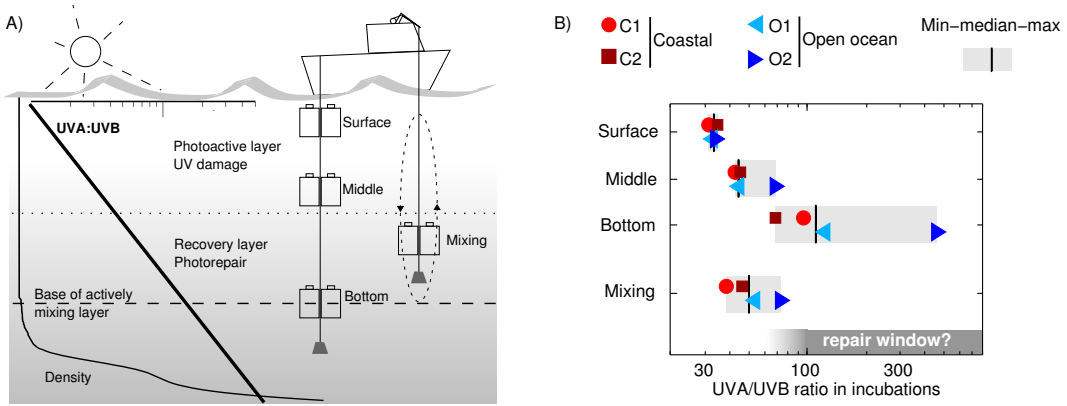

Fig. 1. (A) Cartoon of the experimental design. Vertically-moving and fixed-depth bottles were incubated in a spectral irradiance gradient, depicted by the UVA/UVB ratio. The dotted and the dashed lines represent the depth of the hypothetical photoactive layer and actively mixing layer, respectively; **(B)** UVA/UVB in the different treatments in each experiment. The horizontal bar indicates the UVA/UVB window where photolyase repair of bacterioplankton is more efficient, calculated from underwater UVR profiles according to Kaiser and Herndl (1997).

BGD
10, 8851–8886, 2013

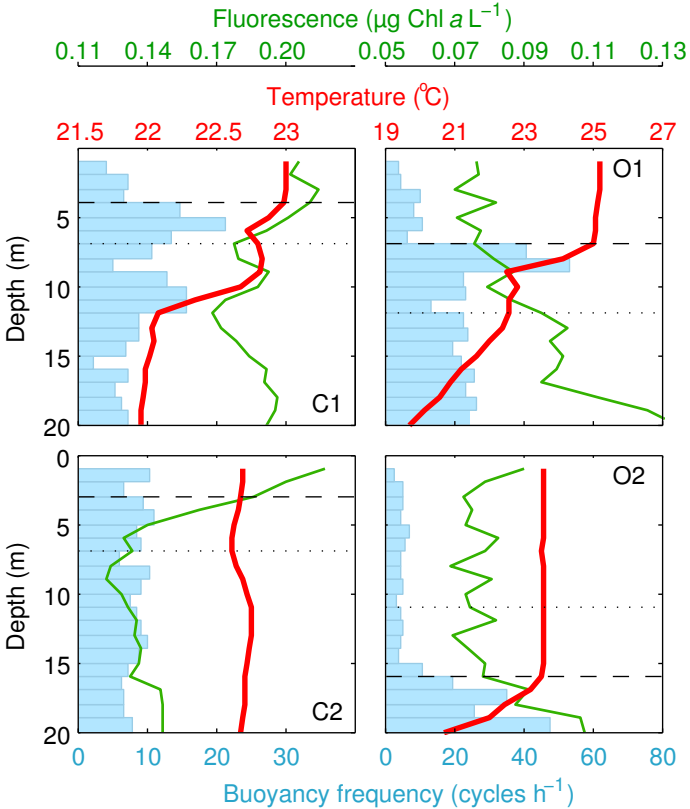

Fig. 2. Vertical profiles of temperature, Chl *a* fluorescence and buoyancy (Brunt–Väisälä) frequency at the time of sampling in the four experiments. The horizontal dashed line indicates the depth of the mixing layer and the dotted line the 10 % penetration of 320 nm radiation.

BGD
10, 8851–8886, 2013

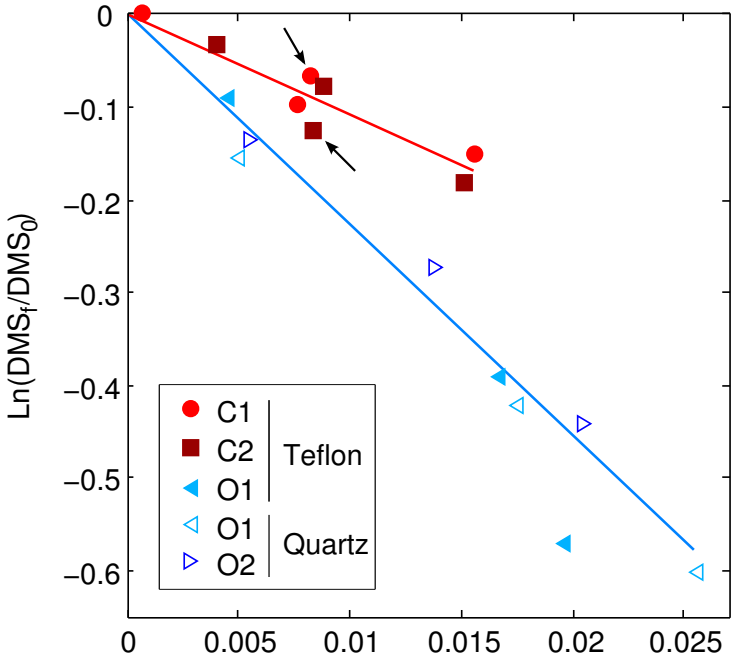

Fig. 3. DMS photolysis in fixed and vertically-moving incubations(DMSf: final DMS concentration; DMS0: initial DMS concentration). The two types of incubation showed consistent dose-response behavior. In C1 and C2 water samples were incubated at three fixed depths and in a vertically-moving basket (marked by arrows), and only initial and final DMS was measured. In O1 and O2 photolysis rates were measured in samples incubated on board and withdrawn at different times. Filled symbols: Teflon bottles. Empty symbols: quartz bottles. The slope of the regression lines is k^*_{photo}: the apparent quantum yield of DMS photolysis with respect to weighted irradiance normalized to 300 nm (as defined by Galí et al., 2013). k^*_{photo} was 22.4 and 11.2 at the coastal station and at the oceanic station, respectively.

BGD
10, 8851–8886, 2013

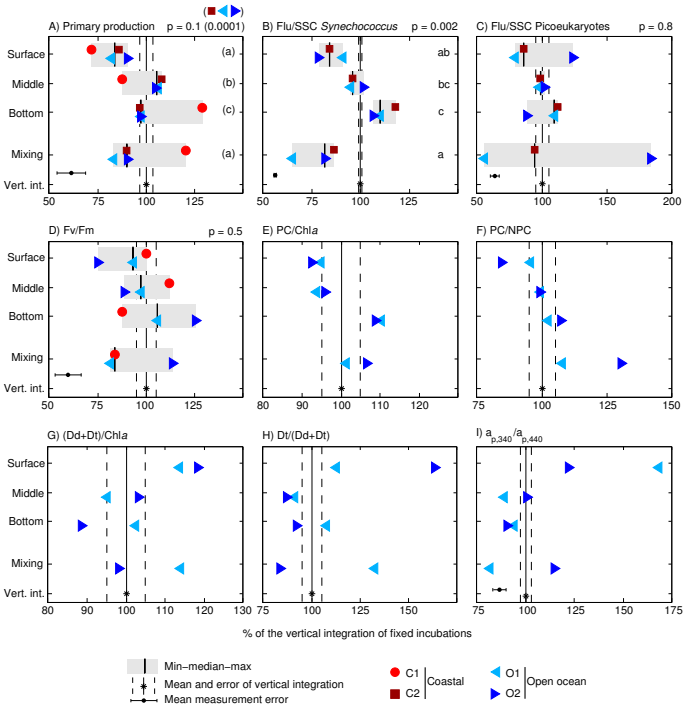

Fig. 4. Response of phytoplankton to irradiance gradients in static and vertically moving incubations. Primary production rates **(A)** and indicators of phytoplankton photoresponse **(B–I)** have been normalized, within each experiment, to the vertical integral of fixed incubations. Flu/SSC: side scatter-normalized cell-specific fluorescence. Fv/Fm: maximum quantum yield of photosystem II photochemistry. PC: photosynthetic carotenoids. NPC: non-photosynthetic carotenoids. Dd: diadinoxanthin. Dt: diatoxanthin. $a_{p,340}/a_{p,440}$: ratio of particulate light absorption coefficient at 340 nm and 440 nm. Differences between treatments are represented by p values of ANOVA tests followed by multiple comparisons (see text for details). In **(A)**, a test was performed on a subset of experiments (C2, O1 and O2) that exhibited a more coherent response.

BGD
10, 8851–8886, 2013

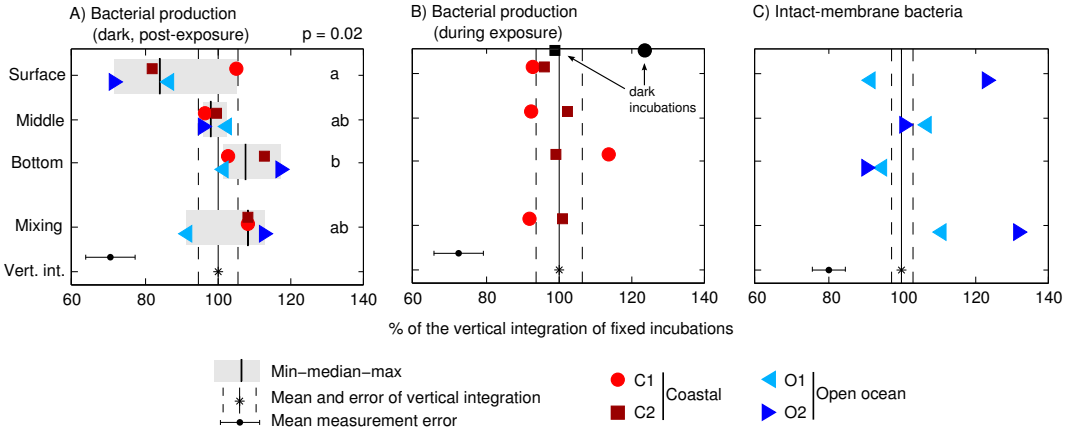

Fig. 5. Response of heterotrophic bacteria to irradiance gradients in static and vertically moving incubations. Leucine incorporation rates in **(A)** post-exposure dark incubations and **(B)** in situ light and dark incubations; **(C)** proportion of intact-membrane ("live") bacteria as deduced from the Nucleic-Acid-Double-Staining (NADS) protocol. Statistical comparisons as in Fig. 4.

BGD
10, 8851–8886, 2013

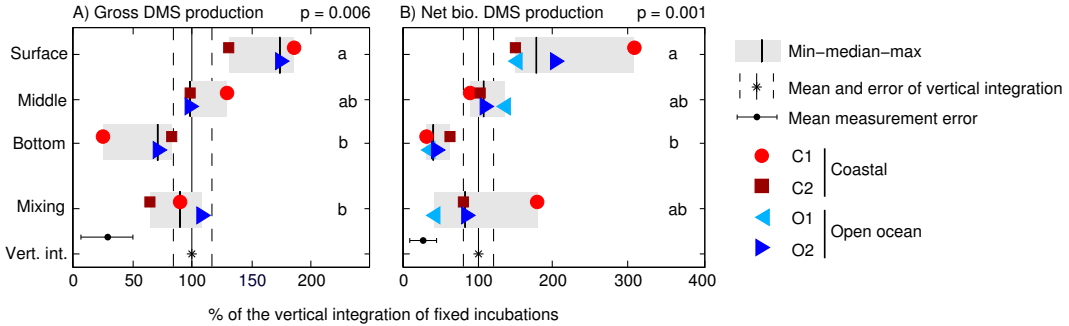

Fig. 6. Response of community DMS production to irradiance gradients in static and vertically moving incubations. **(A)** Gross DMS production (GP_{DMS}, DMDS-amended incubations); **(B)** net biological DMS production (non-amended incubations; equivalent to GP_{DMS} minus bacterial DMS consumption). Statistical comparisons as in Fig. 4.

BGD
10, 8851–8886, 2013

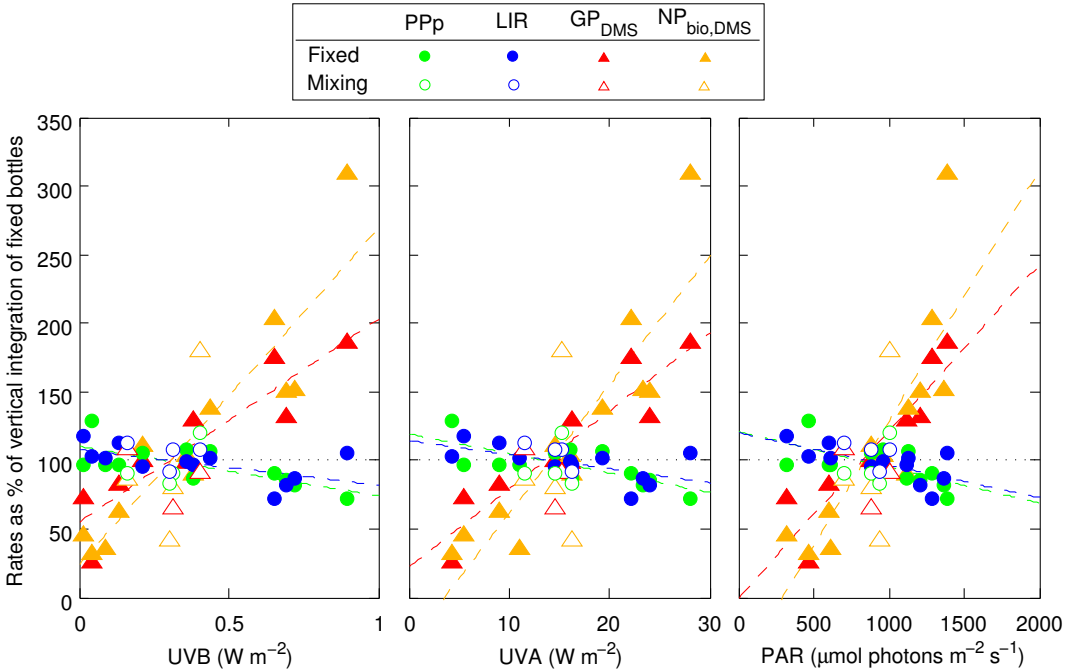

Fig. 7. Relationship between mean UVB, UVA and PAR irradiance during the incubations and particulate primary production (PPp), leucine incorporation rates (LIR), gross DMS production (GP_{DMS}) and net biological DMS production ($NP_{bio,DMS}$). The rates have been normalized to the vertical integral of fixed-depth incubations. The lines represent linear least squares fits to the fixed-depth incubations only (filled symbols). Vertically-moving ("mixing") incubations (open symbols) have not been included in the regressions.

BGD
10, 8851–8886, 2013

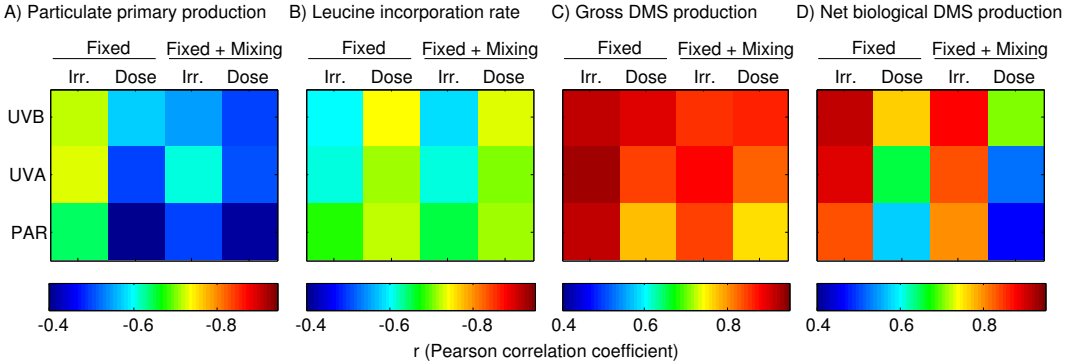

Fig. 8. Pearson correlation coefficient (r) between biogeochemical process rates and mean incubation irradiance (Irr.) or cumulative dose in different radiation bands (UVB, UVA and PAR), in fixed bottles only and in the ensemble of fixed + mixing bottles. Note that r is negative in (**A** and **B**) and positive in (**C** and **D**).

BGD
10, 8851–8886, 2013